Slowing the Time-Fluctuating MIMO Channel by Beam Forming

Dmitry Chizhik

***Abstract*—It has been reported that the number of transmitters that can be used beneficially in a multiple-input multiple-output (MIMO) system is limited by the coherence time of the channel due to difficulties with channel estimation at the receiver. Furthermore, rapid channel fluctuations degrade the performance of feedback schemes that would otherwise increase the information throughput that may be achieved. These impediments either reduce achievable capacity or impose an effective "speed limit" on the mobile, above which the effective throughput is reduced. In this paper, the signal incident at the mobile is represented as a sum of plane waves. The channel transfer matrix is found to factor into time-dependent and time-independent parts. A processing method is proposed whereby the received signals are first preprocessed so as to produce signals that fluctuate on a much slower time scale. The preprocessing consists of beam forming, followed by Doppler compensation for signals received on each beam. Both operations are nonsingular and do not alter the capacity of the MIMO channel. Beam forming effectively partitions the angular spectrum at the mobile, with each partition suffering a smaller Doppler spread, resulting in a "slowed down" channel fluctuation due to mobile motion. The coherence time of the preprocessed channel is found to increase by a factor on the order of the number of mobile receive antennas. In the limit of an infinite number of mobile receive antennas, the MIMO channel is shown to become static. These results remove constraints imposed by training requirements on the number of transmit antennas and increase allowed vehicle speeds. The "slowed down" channel characteristics may also be fed back to the transmitter, allowing an increase in information throughput.**

***Index Terms*—Channel estimation, Doppler, multiple input multiple output (MIMO), time-fluctuation, training.**

I. Introduction

RAPID temporal fluctuations of channel characteristics present fundamental as well as practical difficulties and limitations on reliable communications. In mobile communications, the primary source of rapid channel fluctuations is the motion of the mobile, presumed to be in a vehicle [5]. For coherent reception, the receiver needs an estimate of the channel, usually obtained by transmitting a known training (pilot) signal. To reduce the impact of noise and interference on channel estimation, successive channel estimates are usually time-averaged. Time-averaging, however, introduces distortion in time-varying channels, as the averaging limits tracking of rapidly varying channels. Duration of the training interval is, thus, limited by the coherence time of the channel.

Manuscript received April 17, 2002; revised October 24, 2002, February 21, 2003, April 28, 2003; accepted June 9, 2003. The editor coordinating the review of this paper and approving it for publication is K. B. Lee.

The author is with Lucent Technologies, Bell Laboratories, Holmdel, NJ 07733 USA (e-mail: chizhik@lucent.com).

Digital Object Identifier 10.1109/TWC.2004.833415

In systems using multiple-input multiple-output (MIMO) communications, the channel must be learned from multiple transmitters, exacerbating the difficulties described. It has been reported [1], [2] that the number of transmitters that may be used in MIMO is limited by the coherence time of the channel. In previous investigations, block-fading channels have been considered and the pilot symbols were time-multiplexed with data symbols. It was pointed out that the number of pilot symbols must not be smaller than the number of transmit antennas. As the number of transmit antennas increases, the required number of pilot symbols would exceed the coherence time of the channel before the data symbols are sent. Furthermore, rapid channel fluctuations degrade the performance of feedback schemes that would otherwise increase the information throughput that may be achieved. In the work by Sun *et al.* [4], channel estimation in continuously faded MIMO channels was analyzed. It was found that the accuracy of channel estimation may be improved through linear interpolation of successive channel estimates. Nevertheless, the accuracy was observed to degrade at higher vehicle speeds. Beside the difficulties in accurate channel estimation, rapid temporal fluctuations of the channel require the receiver to adapt to the channel at a rate comparable with the rate of channel fluctuation. Computation of the receiver settings (e.g., space or space-time equalizer settings) demands computational power that increases with the rate of channel fluctuation and the number of transmit antennas.

These difficulties persist in the case of systems where the pilot signals are sent on a separate parallel channel, e.g., a pilot code in code division multiple access (CDMA) [10]. As coherent MIMO communication requires that the channel be learned from every transmitter, the (finite) pilot signal power is split between different transmitters, making an estimate from each more prone to noise and interference. Here, again, duration of the available training period is limited by the coherence time of the channel. Reduction of Doppler spread for a single-input multiple-output (SIMO) channel through a combination of beam forming, followed by Doppler compensation has been proposed by Norklit and Vaughan [16]. There, multiple antennas at the mobile have been used to form beams, with beam signals combined following Doppler compensation. The result was a reduction in fading rate. However, the multiple receive antennas were not used in [16] to combine the received signals coherently, thus resulting in an effective SISO channel with no gain in received power or diversity. The technique proposed in [16] is generalized here for MIMO communications, allowing the full benefit of such systems [17], [18].

It is also noted that in [14] and [20], spectral decomposition of the channel matrix both at the transmitter and at the receiver

has been used to provide insight into channel behavior which is relevant to the current work.

In this paper, the time-varying channel transfer matrix $\mathbf{H}(t)$ is presented in terms of plane waves incident at the mobile. Preprocessing of the signal vector at the mobile is proposed, consisting of beam forming and Doppler compensation for signals received on each beam. Both operations are nonsingular and do not alter the underlying capacity of the MIMO channel. Reduction in the angular spread achieved by beam forming leads to a reduction of the Doppler spread. This is shown to effectively "slow down" the channel fluctuation due to mobile motion. The coherence time of the preprocessed channel is found to increase by a factor on the order of the number of mobile receive antennas. In the limit of an infinite number of mobile receive antennas, the MIMO channel is shown to become static, provided the scatterers also remain static. The preprocessed signals may be treated as signals arriving on virtual antennas, as in [14], and may be further processed in an arbitrary way. This may be capitalized upon both to improve the performance of channel estimation and tracking, as well as to allow feedback to transmitter to increase the throughput.

It is further proposed that the same technique may be used to reduce the rate of channel fluctuation for the mobile-to-base (uplink) communication. To that end, transmitted signals from the mobile are sent along the beams, as opposed to individual antennas. Each signal is precompensated for Doppler prior to beam forming.

The paper is organized as follows. Section II describes the modeling of time-varying $\mathbf{H}$ matrices. Section III describes the receiver preprocessing for the case of an infinite number of mobile antennas. Receiver preprocessing in the case of a finite number of mobile receive antennas is described in Section IV. The resulting increase in coherence time is quantified in Section V. Constraints on optimal number of base transmit antennas are discussed in Section VI. Section VII describes the beam forming at the mobile transmitter, and Section VIII outlines the conclusions.

II. Representation of Time-Varying $\mathbf{H}$ Matrices

The environment being considered is that of a stationary base station, with the mobile moving with constant velocity through clutter. The scatterers are assumed stationary, with the understanding that the dominant source of rapid temporal variation is due to the mobile motion. A casual observation may be made that in terrestrial propagation environments, the most rapidly moving common scatterers are other vehicles, whose physical size is but a small fraction of that of buildings, terrain features, and trees slowly swaying in the wind. When the mobile is moving, however, waves scattered from stationary scatterers are no longer perceived as stationary. A vivid illustration of this may be found in Jakes [5, sec. 1.2.2], where the Doppler spectrum is seen to broaden considerably as the mobile increases its speed.

Here, we will consider only fields in a single particular polarization. The field incident at the mobile may then be regarded as scalar. In the absence of motion, the field E for a particular polarization incident at the mobile antenna located at $\mathbf{r}$ may be represented as a superposition of plane waves

$$E(\mathbf{r}) = \int A(\mathbf{k}) e^{i\mathbf{k}\bullet\mathbf{r}} d\mathbf{k} \tag{1}$$

where $A(\mathbf{k})$ are complex amplitudes of plane waves arriving from the direction corresponding to the wave vector direction $\mathbf{k}$. For a mobile moving with a constant velocity $\mathbf{v}$, the location $\mathbf{r}$ becomes a function of time

$$\mathbf{r}(t) = \mathbf{r}_0 + \mathbf{v}t \tag{2}$$

and the incident field becomes

$$E(\mathbf{r}(t)) = \int d\mathbf{k} A(\mathbf{k}) e^{i\mathbf{k}\bullet\mathbf{r}_0} e^{i\mathbf{k}\bullet\mathbf{v}t} \tag{3}$$

where $\omega_D = \mathbf{k} \bullet \mathbf{v}$ is the Doppler angular frequency. In the case of fields perceived by stationary terminals, any complete orthogonal basis may be used to expand the spatial field in (1), and the choice of the plane wave expansion in (1) is arbitrary and not particularly better than, say, spherical harmonics. In the case of receivers undergoing uniform linear motion (2), however, the plane wave expansion is a natural expansion, as plane waves are eigenfunctions of induced temporal variations, with plane waves remaining uncoupled and each plane wave suffering multiplication by the Doppler factor $e^{i\mathbf{k}\bullet\mathbf{v}t}$, an eigenvalue of the temporal evolution.

Equation (3) may be generalized to the multiple antenna case where the channel is described by a channel matrix $\mathbf{H}$, with an element h_{nm} describing the channel from the transmitter m to receiver n. Although the results below may be generalized to a frequency dependent case, only frequency independent channels will be treated here. The element h_{nm} may be recognized as the Green's function (i.e., point source response) $G(\mathbf{r}_n, \mathbf{r}'_m)$ of the channel, sampled spatially at the receiver location $\mathbf{r}_n$ and the transmitter location $\mathbf{r}'_m$. Like the electric field in (3), the Green's function may be represented formally as a sum of plane waves arriving at a receiver through a Fourier transform with respect to the receiver coordinates

$$G(\mathbf{r}_n(t), \mathbf{r}'_m) = \int d\mathbf{k} A(\mathbf{k}, \mathbf{r}'_m) e^{i\mathbf{k}\bullet\mathbf{r}_n(0)} e^{i\mathbf{k}\bullet\mathbf{v}t} \tag{4}$$

where the receive array is assumed to be moving uniformly, as in (2). The entire narrowband time-dependent channel $\mathbf{H}$ matrix of size $N_R \times N_T$ may then be written as (5), located at the bottom of the following page.

The angular spectrum coefficients $A(\mathbf{k}, \mathbf{r}'_m)$ are the complex amplitudes of plane waves arriving at the mobile receiver from direction of the wave vector $\mathbf{k}$ due to a source at $\mathbf{r}'_m$. Here, N_R and N_T are the number of receive and transmit antennas, respectively. Discretizing the wave vector space $\mathbf{k}$ into a discrete set of N_L plane waves with a step $\Delta\mathbf{k}$, replacing the previous integrals by corresponding sums, and defining $A_m(\mathbf{k}) \triangleq A(\mathbf{k}, \mathbf{r}'_m)$, the $\mathbf{H}$ matrix may be written as (6), located at the bottom of the following page.

Continuous spectral distribution is reached in the limit $N_L \to \infty$. Equation (6) may be factored into

$$\mathbf{H}(t) = \frac{1}{\sqrt{N_L}} \overbrace{\begin{pmatrix} e^{i\mathbf{k_1}\bullet\mathbf{r_1}} & e^{i\mathbf{k_2}\bullet\mathbf{r_1}} & \cdots & e^{i\mathbf{k}_{N_L}\bullet\mathbf{r_1}} \\ e^{i\mathbf{k_1}\bullet\mathbf{r}_2} & e^{i\mathbf{k_2}\bullet\mathbf{r}_2} & \cdots & e^{i\mathbf{k}_{N_L}\bullet\mathbf{r}_2} \\ \vdots & \vdots & \ddots & \vdots \\ e^{i\mathbf{k_1}\bullet\mathbf{r}_{N_R}} & e^{i\mathbf{k_2}\bullet\mathbf{r}_{N_R}} & \cdots & e^{i\mathbf{k}_{N_L}\bullet\mathbf{r}_{N_R}} \end{pmatrix}}^{\mathbf{B}} \times \overbrace{\begin{pmatrix} e^{i\mathbf{k_1}\bullet\mathbf{v}t} & 0 & \cdots & 0 \\ 0 & e^{i\mathbf{k_2}\bullet\mathbf{v}t} & \cdots & 0 \\ \vdots & \vdots & \ddots & \vdots \\ 0 & 0 & \cdots & e^{i\mathbf{k}_{N_L}\bullet\mathbf{v}t} \end{pmatrix}}^{\mathbf{D}} \times \overbrace{\begin{pmatrix} A_1(\mathbf{k}_1) & A_2(\mathbf{k}_1) & \cdots & A_{N_T}(\mathbf{k}_1) \\ A_1(\mathbf{k}_2) & A_2(\mathbf{k}_2) & \cdots & A_{N_T}(\mathbf{k}_2) \\ \vdots & \vdots & \ddots & \vdots \\ A_1(\mathbf{k}_{N_L}) & A_2(\mathbf{k}_{N_L}) & \vdots & A_{N_T}(\mathbf{k}_{N_L}) \end{pmatrix}}^{\mathbf{H_k}} \tag{7}$$

Or, in short hand notation

$$\mathbf{H}(t) = \mathbf{BDH_k} \tag{8}$$

where $\mathbf{H}_k$ is the scattering matrix of the channel, each element of which relates the signal emitted from a particular base antenna to a plane wave incident on the receive antenna array. The diagonal Doppler shift matrix $\mathbf{D}$ represents the time dependent phase evolutions, i.e., Doppler shifts, of the plane waves incident at the receive array. The matrix $\mathbf{B}$ is the inverse spatial Fourier transform matrix, evaluated at receive antenna locations. This matrix depends explicitly on the receive antenna locations, and may be described as an inverse beam forming matrix. As the number N_L of plane waves being summed in (6) is generally infinite, in (7) there are an infinite number of rows in $\mathbf{H}_\mathrm{k}$, columns in $\mathbf{B}$, and both rows and columns in $\mathbf{D}$. The antenna elements considered so far may be placed arbitrarily in space, and not necessarily in a regular linear array. In later numerical examples, the mobile array will be assumed to be a regular linear array. If the mobile array is not located in free space, but rather inside a car, then the matrix $\mathbf{B}$ used above changes form and becomes a coupling matrix, describing the response of each mobile antenna to a plane wave incident at the exterior of the vehicle. It will be assumed here that such near-field effects do not perturb the matrix $\mathbf{B}$ significantly, (viewing the car as mostly transparent), and $\mathbf{B}$ may, therefore, be described as an inverse Fourier transform matrix, as in (7). The channel scattering matrix $\mathbf{H}_\mathrm{k}$ is equivalent to a spatial Fourier transform of the Green's function of the channel with respect to the mobile receiver (here stationary) coordinates:

$$\mathbf{H}_\mathrm{k}(\mathbf{k}, \mathbf{r}') = \int d\mathbf{r} G(\mathbf{r}_0, \mathbf{r}') e^{-i\mathbf{k}\bullet\mathbf{r}_0}. \tag{9}$$

The $\mathbf{H}_\mathrm{k}$ matrix is thus characteristic of the channel and is independent of the receiver array design. It is assumed in this work that the scatterers are not moving, thus both the Green's function $G(\mathbf{r}_0, \mathbf{r}')$ in (9) and the matrix $\mathbf{H}_\mathrm{k}$ in (7) and (9) are not dependent on time. The Green's function in (9) is the same as the Green's function in (4), evaluated at $t = 0$. Furthermore, large scale variations in time due to, say, vehicle moving into a different environment in the next street are not included, leading to the angular spectra $A_m(\mathbf{k})$ in (7) remaining independent of time. The representation of the $\mathbf{H}$ matrix used in (6) and (7) is simply a factorization of a general $\mathbf{H}$ matrix, with the noted restriction that the temporal variation is only a consequence of linear uniform motion of the mobile, as described earlier. No other restrictions are imposed. In particular, the entries of the $\mathbf{H}$ matrix may be distributed as correlated complex Gaussian random variables, as is often assumed [17], or may be non-Gaussian as in the case of the keyhole channel [6]. To generate a Gaussian distributed $\mathbf{H}$ matrix with correlations at the receiver stemming from a limited angular spread, the angular spectra $A(\mathbf{k})$ may be generated as complex Gaussian independent identically distributed (i.i.d.). variables, which are then weighted so as to produce an angular spectrum of desired shape. To introduce correlations at the transmitter, the $\mathbf{H}$ matrix may be multiplied from the right by an appropriate transformation [11]–[13]. In this work, no assumptions of the distribution

$$\mathbf{H}(t) = \begin{pmatrix} \int_{-\infty}^{\infty} d\mathbf{k} A(\mathbf{k}, \mathbf{r}'_\mathbf{1}) e^{i\mathbf{k}\bullet\mathbf{r}_1} e^{i\mathbf{k}\bullet\mathbf{v}t} & \int_{-\infty}^{\infty} d\mathbf{k} A(\mathbf{k}, \mathbf{r}'_2) e^{i\mathbf{k}\bullet\mathbf{r}_1} e^{i\mathbf{k}\bullet\mathbf{v}t} & \cdots & \int_{-\infty}^{\infty} d\mathbf{k} A(\mathbf{k}, \mathbf{r}'_{N_T}) e^{i\mathbf{k}\bullet\mathbf{r}_1} e^{i\mathbf{k}\bullet\mathbf{v}t} \\ \int_{-\infty}^{\infty} d\mathbf{k} A(\mathbf{k}, \mathbf{r}'_\mathbf{1}) e^{i\mathbf{k}\bullet\mathbf{r}_2} e^{i\mathbf{k}\bullet\mathbf{v}t} & \int_{-\infty}^{\infty} d\mathbf{k} A(\mathbf{k}, \mathbf{r}'_2) e^{i\mathbf{k}\bullet\mathbf{r}_2} e^{i\mathbf{k}\bullet\mathbf{v}t} & \cdots & \int_{-\infty}^{\infty} d\mathbf{k} A\left(\mathbf{k}, \mathbf{r}'_{N_T}\right) e^{i\mathbf{k}\bullet\mathbf{r}_2} e^{i\mathbf{k}\bullet\mathbf{v}t} \\ \vdots & \vdots & \ddots & \vdots \\ \int_{-\infty}^{\infty} d\mathbf{k} A(\mathbf{k}, \mathbf{r}'_\mathbf{1}) e^{i\mathbf{k}\bullet\mathbf{r}_{N_R}} e^{i\mathbf{k}\bullet\mathbf{v}t} & \int_{-\infty}^{\infty} d\mathbf{k} A(\mathbf{k}, \mathbf{r}'_2) e^{i\mathbf{k}\bullet\mathbf{r}_{N_R}} e^{i\mathbf{k}\bullet\mathbf{v}t} & \cdots & \int_{-\infty}^{\infty} d\mathbf{k} A\left(\mathbf{k}, \mathbf{r}'_{N_T}\right) e^{i\mathbf{k}\bullet\mathbf{r}_{N_R}} e^{i\mathbf{k}\bullet\mathbf{v}t} \end{pmatrix} \tag{5}$$

$$\mathbf{H}(t) = \frac{1}{\sqrt{N_L}} \begin{pmatrix} \sum_l A_1(\mathbf{k}_l) e^{i\mathbf{k}_l\bullet\mathbf{r}_1} e^{i\mathbf{k}_l\bullet\mathbf{v}t} & \sum_l A_2(\mathbf{k}_l) e^{i\mathbf{k}_l\bullet\mathbf{r}_1} e^{i\mathbf{k}_l\bullet\mathbf{v}t} & \cdots & \sum_l A_{N_T}(\mathbf{k}_l) e^{i\mathbf{k}_l\bullet\mathbf{r}_1} e^{i\mathbf{k}_l\bullet\mathbf{v}t} \\ \sum_l A_1(\mathbf{k}_l) e^{i\mathbf{k}_l\bullet\mathbf{r}_2} e^{i\mathbf{k}_l\bullet\mathbf{v}t} & \sum_l A_2(\mathbf{k}_l) e^{i\mathbf{k}_l\bullet\mathbf{r}_2} e^{i\mathbf{k}_l\bullet\mathbf{v}t} & \cdots & \sum_l A_{N_T}(\mathbf{k}_l) e^{i\mathbf{k}_l\bullet\mathbf{r}_2} e^{i\mathbf{k}_l\bullet\mathbf{v}t} \\ \vdots & \vdots & \ddots & \vdots \\ \sum_l A_1(\mathbf{k}_l) e^{i\mathbf{k}_l\bullet\mathbf{r}_{N_R}} e^{i\mathbf{k}_l\bullet\mathbf{v}t} & \sum_l A_2(\mathbf{k}_l) e^{i\mathbf{k}_l\bullet\mathbf{r}_{N_R}} e^{i\mathbf{k}_l\bullet\mathbf{v}t} & \cdots & \sum_l A_{N_T}(\mathbf{k}_l) e^{i\mathbf{k}_l\bullet\mathbf{r}_{N_R}} e^{i\mathbf{k}_l\bullet\mathbf{v}t} \end{pmatrix} \tag{6}$$

of the $\mathbf{H}$ matrix entries is made, and the results are independent of the spatial model.

The previous model may be modified by carrying out a similar expansion of the field at the base transmitter. By analogy to (6), an element of the $\mathbf{H}$ matrix may be written as a superposition of N_L plane waves at the mobile, coupled to N_L plane waves launched from the base through a scattering matrix $S(\mathbf{k}_l^{\mathrm{MS}}, \mathbf{k}_s^{\mathrm{BS}})$ as in [14]

$$h_{nm}(t) = \frac{1}{N_L} \sum_{s=1}^{N_L} \sum_{l=1}^{N_L} S\left(\mathbf{k}_l^{\mathrm{MS}}, \mathbf{k}_s^{\mathrm{BS}}\right) \times e^{i\mathbf{k}_l^{\mathrm{MS}} \bullet \mathbf{r}_n^{\mathrm{MS}}} e^{i\mathbf{k}_l^{\mathrm{MS}} \bullet \mathbf{v}t} e^{i\mathbf{k}_s^{\mathrm{BS}} \bullet \mathbf{r}_m^{\mathrm{BS}}}. \quad (10)$$

The superscripts MS and BS refer to mobile and base, respectively. The scattering matrix $S(\mathbf{k}_l^{\mathrm{MS}}, \mathbf{k}_s^{\mathrm{BS}})$ may be interpreted as a discrete version of a double Fourier transform of the Green's function $G(\mathbf{r}^{\mathrm{MS}}, \mathbf{r}^{\mathrm{BS}})$ with respect to both mobile coordinates $\mathbf{r}^{\mathrm{MS}}$ and base coordinates $\mathbf{r}^{\mathrm{BS}}$. Such representation is one of an infinite set of possible orthogonal expansions of the field. The channel representation used in (10) may be written formally as a single summation over "paths" [15], as discussed in [14], each with a particular departure and arrival direction. Certain exceptional channels may be constructed, where each path has a unique departure and arrival direction, as for example, in the case of single scattering from specular scatterers. This would lead to the scattering matrix $S(\mathbf{k}_l^{\mathrm{MS}}, \mathbf{k}_s^{\mathrm{BS}})$ becoming diagonal, which is one of the cases explored in [14]. In general, a plane wave launched from the base results in multiple plane waves arriving at the terminal from a plurality of angles. This may be seen from (10), as a launching of a plane wave in the direction of $\mathbf{k}_s^{\mathrm{BS}} = \mathbf{k}_{s_1}^{\mathrm{BS}}$ from the base would result in a channel response that is proportional to

$$\sum_{l=1}^{N_L} S\left(\mathbf{k}_l^{\mathrm{MS}}, \mathbf{k}_{s_1}^{\mathrm{BS}}\right) e^{i\mathbf{k}_l^{\mathrm{MS}} \bullet \mathbf{r}_n^{\mathrm{MS}}} e^{i\mathbf{k}_l^{\mathrm{MS}} \bullet \mathbf{v}t}. \quad (11)$$

This would result in observed spread of Doppler frequencies $\omega_l^D = \mathbf{k}_l^{\mathrm{MS}} \bullet \mathbf{v}t$ that is, in general, undiminished even if the base array can synthesize such a plane wave signal. In contrast, a single plane wave at the mobile in the direction $\mathbf{k}_l^{\mathrm{MS}} = \mathbf{k}_{l_1}^{\mathrm{MS}}$ results in the channel response proportional to

$$e^{i\mathbf{k}_{l_1}^{\mathrm{MS}} \bullet \mathbf{r}_n^{\mathrm{MS}}} e^{i\mathbf{k}_{l_1}^{\mathrm{MS}} \bullet \mathbf{v}t} \sum_{s=1}^{N_L} S\left(\mathbf{k}_{l_1}^{\mathrm{MS}}, \mathbf{k}_s^{\mathrm{BS}}\right) e^{i\mathbf{k}_s^{\mathrm{BS}} \bullet \mathbf{r}_m^{\mathrm{BS}}} = A_m\left(\mathbf{k}_{l_1}^{\mathrm{MS}}\right) e^{i\mathbf{k}_{l_1}^{\mathrm{MS}} \bullet \mathbf{r}_n^{\mathrm{MS}}} e^{i\mathbf{k}_{l_1}^{\mathrm{MS}} \bullet \mathbf{v}t} \quad (12)$$

where the last equality follows from (6). Now the temporal evolution contains a single Doppler shifted term, as opposed to a sum of Doppler shifted terms in (11). As the base is normally stationary, plane wave expansions at the base do not offer the same unique advantages as they do in the case of similar expansion at the mobile, where they form a set of temporal eigenfunctions. Angular spectrum representation at the base is, therefore, not considered in this work. In cases where particular clusters of scatterers are visible both from the base and from the mobile [19], beam forming at the base may prove beneficial. It should also be noted that in cases where there is limited angle spread at the base, statistical description of the channel may be more naturally expressed in the angular spectrum basis.

III. Receiver Processing for an Infinite Number of Mobile Antennas

As the number of mobile antennas N_R increases, the angular resolution of the mobile array increases, and the array begins to resolve individual plane waves in the limit of infinite number of antennas, and given a finite set of N_L distinct plane waves. In that limit, the columns of the inverse Fourier transform matrix $\mathbf{B}$ become orthogonal (see (13), located at the bottom of the page) where $\mathbf{I}$ is the identity matrix of size N_L, and the dagger symbol denotes the Hermitian transpose. Here, spacing between neighboring antennas remains fixed (and assumed to be 0.5λ), thus the increase in the number of antennas leads to an increase in the mobile antenna effective aperture. The orthogonality of the rows of $\mathbf{B}$ holds in the limit of infinite number of mobile antennas, provided the number of distinct plane waves is large but finite while the number of mobile antennas approaches infinity. The restriction on the number of plane waves is used here but removed in the rest of the work. This causes the matrix $\mathbf{B}$ to have an increasing number N_R of rows, while keeping a constant number of columns N_L. The rank of $\mathbf{H}$ is, therefore, constrained not to exceed N_L by assumption. Alternatively, the set of wave vectors $\mathbf{k}$ used in defining $\mathbf{B}$ may be constructed so as to make $\mathbf{B}$ a discrete Fourier transform (DFT) matrix, which is unitary by construction [14]. The Doppler matrix $\mathbf{D}$ in (7) is evidently unitary. Using (13), the time evolution of the $\mathbf{H}$ matrix in the limit of infinite number of mobile antennas may be represented as

$$\mathbf{H}(t) = \mathbf{B}\mathbf{D}(\mathbf{v}t)\mathbf{H}_{\mathrm{k}} = \mathbf{B}\mathbf{D}(\mathbf{v}t)\frac{N_L}{N_R}\mathbf{B}^{\dagger}\mathbf{H}(0) = \mathbf{U}(\mathbf{v}t)\mathbf{H}(0) \quad (14)$$

$$\lim_{N_R \to \infty} \frac{1}{N_R}\mathbf{B}^{\dagger}\mathbf{B} = \lim_{N_R \to \infty} \frac{1}{N_R}\frac{N_R}{N_L} \begin{pmatrix} 1 & \frac{1}{N_R}\sum_{n=1}^{N_R} e^{i(\mathbf{k}_2 - \mathbf{k}_1)\bullet \mathbf{r}_n} & \cdots & \frac{1}{N_R}\sum_{n=1}^{N_R} e^{i(\mathbf{k}_{N_L} - \mathbf{k}_1)\bullet \mathbf{r}_n} \\ \frac{1}{N_R}\sum_{n=1}^{N_R} e^{i(\mathbf{k}_1 - \mathbf{k}_2)\bullet \mathbf{r}_n} & 1 & \cdots & \frac{1}{N_R}\sum_{n=1}^{N_R} e^{i(\mathbf{k}_{N_L} - \mathbf{k}_2)\bullet \mathbf{r}_n} \\ \vdots & \vdots & \ddots & \vdots \\ \frac{1}{N_R}\sum_{n=1}^{N_R} e^{i(\mathbf{k}_1 - \mathbf{k}_{N_L})\bullet \mathbf{r}_n} & \frac{1}{N_R}\sum_{n=1}^{N_R} e^{i(\mathbf{k}_2 - \mathbf{k}_{N_L})\bullet \mathbf{r}_n} & \cdots & 1 \end{pmatrix} = \frac{1}{N_L}\mathbf{I} \quad (13)$$

where the temporal evolution operator

$$\mathbf{U}(\mathbf{v}t) = \frac{N_L}{N_R}\mathbf{B}\mathbf{D}(\mathbf{v}t)\mathbf{B}^{\dagger}. \tag{15}$$

The connection between angular and temporal spectra is well known and has been used to derive fading statistics both theoretically [5] and in processing of measurements [8], [9]. In a practical receiver, the channel matrix $\mathbf{H}(t)$ must be estimated, usually from pilot or training signals. For a rapidly time varying channel, the channel must be determined at frequent intervals. While this is true in a general time-varying channel, the structure (7) of temporal evolution of the $\mathbf{H}(\mathrm{t})$ matrix may be exploited. In fact, if the channel is known at time $t = 0$, it may be determined at a later time t through applying the evolution operators (15) in (14). Note that the evolution operators are not functions of the environment in a sense that the proper inverse beam forming matrix $\mathbf{B}$ is defined by the array geometry and the immediate vicinity of the mobile array (e.g., interior of a car). Similarly, the Doppler shift matrix $\mathbf{D}$ depends on vehicle velocity alone. Alternatively, the receiver processing may include the evolution of the $\mathbf{H}$ matrix explicitly. The vector of received signals $\mathbf{r}$ in a MIMO system is related to the transmitted signal vector $\mathbf{s}$

$$\mathbf{r} = \mathbf{H}(t)\mathbf{s} + \mathbf{n} = \frac{N_L}{N_R}\mathbf{B}\mathbf{D}(\mathbf{v}t)\mathbf{B}^{\dagger}\mathbf{H}(0)\mathbf{s} + \mathbf{n} \tag{16}$$

where $\mathbf{n}$ is the vector of received noise signals. A vector of virtual receiver signals $\mathbf{r}''$ may be constructed by applying a sequence of operations to the received signal

$$\mathbf{r}'' = \mathbf{D}^{\dagger}(\mathbf{v}t)\mathbf{B}^{\dagger}\mathbf{r} = \mathbf{B}^{\dagger}\mathbf{H}(0)\mathbf{s} + \mathbf{n}' \tag{17}$$

where $\mathbf{n}'$ is the equivalent receiver noise. The rank of both $\mathbf{B}^{\dagger}$ and $\mathbf{H}(0)$ may not exceed N_L. Note that the transformed received signal $\mathbf{r}''$ is related to the transmitted signal through a nontime varying channel. The capacity of such a channel is, therefore, constant with time as well. This is utilized in the following for the more practical case of a finite number of receivers at the mobile and no restriction on the number of plane waves present.

IV. Receiver Processing for Finite Number of Mobile Antennas

In the case of a finite number of antennas, (7) still applies, but the transformation $\mathbf{B}^{\dagger}$ used in (16) does not generally have orthogonal rows. It is known, however, that any nonsingular transformation of the received signal vector does not alter capacity, because the same transformation is applied both to the desired signal and noise. In particular, a set of N_K distinct beams may be formed at the receiver in directions given by a set of vectors $\mathbf{K}_1, \mathbf{K}_2, \ldots \mathbf{K}_{N_K}$. Applying the beam forming transformation $\mathbf{B}_1^{\dagger}$ (see (18), located at the the bottom of the page) to the receive signal vector $\mathbf{r} = \mathbf{H}(t)\mathbf{s} + \mathbf{n}$, a vector of virtual received signals $\mathbf{r}'$ is constructed (see (19), located at the bottom of the page) where the complex amplitude response G of the receive array to the plane wave arriving from direction $\mathbf{k}$ is defined as

$$G(\mathbf{k} - \mathbf{K_p}) = \frac{1}{\sqrt{N_R}}\sum_{n=1}^{N_R} e^{-i(\mathbf{k}-\mathbf{K}_p)\cdot\mathbf{r}_n} \tag{20}$$

when the receive antenna elements are phased so as to produce a maximum in the direction $\mathbf{K_p}$. Note that $G(0) = \sqrt{N_R}$. The directions of $\mathbf{K_p}$ may be chosen so as to make (18) unitary. For example, in the case of a uniform linear array of N_R mobile antennas, separated by $d = \lambda/2$, the x-component of $\mathbf{K_p}$ along the line of the array would be given by $K_x = (2\pi)/(N_R d)[-N_R/2 + 1, -N_R/2 + 2, \ldots, N_R/2]$. $\mathbf{B}_1^{\dagger}$ is an $N_K \times N_R$ matrix, where N_K is the number of beam outputs. The number of information bearing receive signals is N_R and, therefore, the rank of the beam forming matrix $\mathbf{B}_1^{\dagger}$ must not be smaller than N_R, thus $N_K \geq N_R$. It should be noted, however, that as these beam signals are formed from a combination of N_R receive antenna signals, no additional information may be obtained if $N_K > N_R$. In dealing with a time-varying channel, however, there may be practical advantages to forming a number of receive beams greater than the number of receive antennas.

Changing variables, (19) may be rewritten as (21), located at the bottom of the followng page.

$$\mathbf{B}_1^{\dagger} = \frac{1}{\sqrt{N_R}}\begin{pmatrix} e^{-i\mathbf{K}_1\bullet\mathbf{r}_1} & e^{-i\mathbf{K}_1\bullet\mathbf{r}_2} & \cdots & e^{-i\mathbf{K}_1\bullet\mathbf{r}_{N_R}} \\ e^{-i\mathbf{K}_2\bullet\mathbf{r}_1} & e^{-i\mathbf{K}_2\bullet\mathbf{r}_2} & \cdots & e^{-i\mathbf{K}_2\bullet\mathbf{r}_{N_R}} \\ \vdots & \vdots & \ddots & \vdots \\ e^{-i\mathbf{K}_{N_K}\bullet\mathbf{r}_1} & e^{-i\mathbf{K}_{N_K}\bullet\mathbf{r}_2} & \cdots & e^{-i\mathbf{K}_{N_K}\bullet\mathbf{r}_{N_R}} \end{pmatrix} \tag{18}$$

$$\mathbf{r}' = \frac{1}{\sqrt{N_L}}\begin{pmatrix} \sum_{\mathbf{k}} A_1(\mathbf{k})G(\mathbf{k}-\mathbf{K_1})e^{i\mathbf{k}\bullet\mathbf{v}t} & \sum_{k} A_2(\mathbf{k})G(\mathbf{k}-\mathbf{K_1})e^{i\mathbf{k}\bullet\mathbf{v}t} & \cdots & \sum_{\mathbf{k}} A_{N_T}(\mathbf{k})G(\mathbf{k}-\mathbf{K_1})e^{i\mathbf{k}\bullet\mathbf{v}t} \\ \sum_{\mathbf{k}} A_1(\mathbf{k})G(\mathbf{k}-\mathbf{K}_2)e^{i\mathbf{k}\bullet\mathbf{v}t} & \sum_{\mathbf{k}} A_2(\mathbf{k})G(\mathbf{k}-\mathbf{K}_2)e^{i\mathbf{k}\bullet\mathbf{v}t} & \cdots & \sum_{\mathbf{k}} A_{N_T}(\mathbf{k})G(\mathbf{k}-\mathbf{K}_2)e^{i\mathbf{k}\bullet\mathbf{v}t} \\ \vdots & \vdots & \ddots & \vdots \\ \sum_{\mathbf{k}} A_1(\mathbf{k})G(\mathbf{k}-\mathbf{K}_{N_K})e^{i\mathbf{k}\bullet\mathbf{v}t} & \sum_{\mathbf{k}} A_2(\mathbf{k})G(\mathbf{k}-\mathbf{K}_{N_K})e^{i\mathbf{k}\bullet\mathbf{v}t} & \cdots & \sum_{\mathbf{k}} A_{N_T}(\mathbf{k})G(\mathbf{k}-\mathbf{K}_{N_K})e^{i\mathbf{k}\bullet\mathbf{v}t} \end{pmatrix}\mathbf{s} + \mathbf{B}_1^{\dagger}\mathbf{n} \tag{19}$$

One can approximate $G(\mathbf{k})$ as being $G_0\sqrt{N_R}$ within the half-power beam width B_h, and zero outside this beam width, where G_0 is a scale factor chosen so that $\int d\Omega |G(\mathbf{k})|^2 = 1$ over all solid angles. Equation (21) may then be rewritten approximately as (22), located at the bottom of the page, where k_x is the component of the wave vector $\mathbf{k}$ along an arbitrary x axis, which may be chosen to be along the line of the array in the case of a uniform linear array.

The half-power beam width B_h near the broadside direction (in spatial frequency units m^{-1}) for a uniformly spaced linear array with antenna spacing d, is given by [7]

$$B_h = 0.886k\frac{\lambda}{N_R d} = 0.886\frac{2\pi}{N_R d}. \tag{23}$$

For example, a four-element array with elements spaced $\lambda/2$ can generate a beam about 25° wide. Linear arrays with azimuthally omnidirectional elements will experience front-back ambiguity. It will be assumed here that the array elements are mounted on the back plane of the mobile terminal, thereby eliminating the front-back ambiguity and making (22) appropriate. For a large number of mobile antennas, the antennas may be placed in a planar grid array, where proper spacing will reduce the front-back ambiguity. The beam forming transformation (18) produces virtual directional antenna responses (22), each pointing into a different direction, with generally some overlap between the beams. The channel induced time fluctuation of each beam is separated into a mean Doppler frequency shift, represented by the diagonal Doppler matrix $\mathbf{D}_1$ in (22) and a "slower" residual time fluctuations given by the $e^{i\mathbf{k}\bullet\mathbf{v}t}$ terms in the second matrix factor in (22), for $|k_x| < B_h/2$.

As is done in conventional receivers, the receiver on each beam would attempt to estimate the channel from the mth transmit antenna, perhaps by correlating the received signal with the corresponding pilot signal. Such a procedure produces a sequence in time of channel estimates of the actual channel coefficient

$$\begin{aligned} h_{nm}(t) &= e^{i\mathbf{K}_n\bullet\mathbf{v}t}\frac{G_0\sqrt{N_R}}{\sqrt{N_L}}\sum_{k_x=-B_h/2}^{k_x=B_h/2} A_m(\mathbf{k}+\mathbf{K_1})e^{i\mathbf{k}\bullet\mathbf{v}t} \\ &= e^{i\omega_n t}h_{nm}^{\text{lowpass}}(t) \end{aligned} \tag{24}$$

as follows from (22). The channel coefficient is seen to have the structure of a band pass signal, whose center frequency is the mean Doppler shift $\omega_n = \mathbf{K}_n \cdot \mathbf{v}$ suffered by the nth beam, which may be observed as a phase drift across the sequence of channel estimates on the nth receive beam. The estimation of the mean Doppler shift ω_n on each beam is then a problem of estimating the center frequency of a band pass process, which may be done, for example, by carrying out a linear least mean squares fit to the phase of the estimates of channel coefficient (24). Thus, while the Doppler shifts ω_n depend on the mobile velocity, the velocity need not be estimated explicitly. Given an estimate of the mean Doppler shift for each beam, a Doppler compensating matrix $\mathbf{D}_\mathbf{1}^\dagger(\mathbf{v}t)$ may be formed and applied to the virtual received signal $\mathbf{r}\prime$, see (25), located at the bottom of

$$\begin{aligned} \mathbf{r}' = &\begin{pmatrix} e^{i\mathbf{K_1}\bullet\mathbf{v}t} & 0 & \cdots & 0 \\ 0 & e^{i\mathbf{K}_2\bullet\mathbf{v}t} & \cdots & 0 \\ \vdots & \vdots & \ddots & \vdots \\ 0 & 0 & \cdots & e^{i\mathbf{K}_{N_K}\bullet\mathbf{v}t} \end{pmatrix}\frac{1}{\sqrt{N_L}} \\ &\times\begin{pmatrix} \sum_{\mathbf{k}} A_1(\mathbf{k}+\mathbf{K_1})G(\mathbf{k})e^{i\mathbf{k}\bullet\mathbf{v}t} & \sum_{\mathbf{k}} A_2(\mathbf{k}+\mathbf{K_1})G(\mathbf{k})e^{i\mathbf{k}\bullet\mathbf{v}t} & \cdots & \sum_{\mathbf{k}} A_{N_T}(\mathbf{k}+\mathbf{K_1})G(\mathbf{k})e^{i\mathbf{k}\bullet\mathbf{v}t} \\ \sum_{\mathbf{k}} A_1(\mathbf{k}+\mathbf{K}_2)G(\mathbf{k})e^{i\mathbf{k}\bullet\mathbf{v}t} & \sum_{\mathbf{k}} A_2(\mathbf{k}+\mathbf{K}_2)G(\mathbf{k})e^{i\mathbf{k}\bullet\mathbf{v}t} & \cdots & \sum_{\mathbf{k}} A_{N_T}(\mathbf{k}+\mathbf{K}_2)G(\mathbf{k})e^{i\mathbf{k}\bullet\mathbf{v}t} \\ \vdots & \vdots & \ddots & \vdots \\ \sum_{\mathbf{k}} A_1\left(\mathbf{k}+\mathbf{K}_{N_K}\right)G(\mathbf{k})e^{i\mathbf{k}\bullet\mathbf{v}t} & \sum_{\mathbf{k}} A_2\left(\mathbf{k}+\mathbf{K}_{N_K}\right)G(\mathbf{k})e^{i\mathbf{k}\bullet\mathbf{v}t} & \cdots & \sum_{\mathbf{k}} A_{N_T}\left(\mathbf{k}+\mathbf{K}_{N_K}\right)G(\mathbf{k})e^{i\mathbf{k}\bullet\mathbf{v}t} \end{pmatrix}\mathbf{s} \\ &+\mathbf{B}_\mathbf{1}^\dagger\mathbf{n} \end{aligned} \tag{21}$$

$$\begin{aligned} \mathbf{r}' \approx &\overbrace{\begin{pmatrix} e^{i\mathbf{K_1}\bullet\mathbf{v}t} & 0 & \cdots & 0 \\ 0 & e^{i\mathbf{K}_2\bullet\mathbf{v}t} & \vdots & 0 \\ \vdots & \vdots & \ddots & \vdots \\ 0 & 0 & \cdots & e^{i\mathbf{K}_{N_K}\bullet\mathbf{v}t} \end{pmatrix}}^{D_1}\frac{G_0\sqrt{N_R}}{\sqrt{N_L}} \\ &\times\begin{pmatrix} \sum_{k_x=-B_h/2}^{k_x=B_h/2} A_1(\mathbf{k}+\mathbf{K_1})e^{i\mathbf{k}\bullet\mathbf{v}t} & \sum_{k_x=-B_h/2}^{k_x=B_h/2} A_2(\mathbf{k}+\mathbf{K_1})e^{i\mathbf{k}\bullet\mathbf{v}t} & \cdots & \sum_{k_x=-B_h/2}^{k_x=B_h/2} A_{N_T}(\mathbf{k}+\mathbf{K_1})e^{i\mathbf{k}\bullet\mathbf{v}t} \\ \sum_{k_x=-B_h/2}^{k_x=B_h/2} A_1(\mathbf{k}+\mathbf{K}_2)e^{i\mathbf{k}\bullet\mathbf{v}t} & \sum_{k_x=-B_h/2}^{k_x=B_h/2} A_2(\mathbf{k}+\mathbf{K}_2)e^{i\mathbf{k}\bullet\mathbf{v}t} & \cdots & \sum_{k_x=-B_h/2}^{k_x=B_h/2} A_{N_T}(\mathbf{k}+\mathbf{K}_2)e^{i\mathbf{k}\bullet\mathbf{v}t} \\ \vdots & \vdots & \ddots & \vdots \\ \sum_{k_x=-B_h/2}^{k_x=B_h/2} A_1\left(\mathbf{k}+\mathbf{K}_{N_K}\right)e^{i\mathbf{k}\bullet\mathbf{v}t} & \sum_{k_x=-B_h/2}^{k_x=B_h/2} A_2\left(\mathbf{k}+\mathbf{K}_{N_K}\right)e^{i\mathbf{k}\bullet\mathbf{v}t} & \cdots & \sum_{k_x=-B_h/2}^{k_x=B_h/2} A_{N_T}\left(\mathbf{k}+\mathbf{K}_{N_K}\right)e^{i\mathbf{k}\bullet\mathbf{v}t} \end{pmatrix}\mathbf{s} \\ &+\mathbf{B}_\mathbf{1}^\dagger\mathbf{n} \end{aligned} \tag{22}$$

the page. Equation (25) may be interpreted as an equivalent received signal, with "slower" time fluctuations, characterized by the Doppler bandwidth

$$\Delta f = \frac{B_h \mathrm{v}}{2\pi} = \frac{1.8\mathrm{v}}{N_R \lambda} \tag{26}$$

where (23) was used. Note that the Doppler bandwidth is inversely proportional to the number of mobile antennas. More frequently, coherence time is used as a measure of temporal scale of channel fluctuations, as discussed in the next section.

As the "slowing" of the channel is achieved by a sequence of nonsingular operators, capacity of the effective channel experienced by the virtual received signal (25), has not been changed by the beam forming and Doppler compensation. This procedure has been demonstrated in computer simulations of a time-varying MIMO link in the presence of noise, as will be reported in a later publication.

The previous "slowing down" procedure requires only an estimate of the mean Doppler shifts per beam to define the diagonal Doppler compensation matrix $\mathbf{D}_\mathbf{1}^\dagger$ in (25). The beam forming matrix $\mathbf{B}_\mathbf{1}^\dagger$ may be formulated for an arbitrary set of distinct beams, a procedure that requires only the knowledge of the relative disposition of the mobile array elements, independent both of the array orientation and the incident angular spectrum.

Due to the multiple scattering, beam forming at the base does not, in general, lead to a reduction in the width of the angular spectrum perceived at the terminal, and thus, no reduction in Doppler bandwidth, as discussed in Section II.

The technique described earlier does not rely on any particular spatial distribution of scatterers. In particular, no assumption of clustering of scatterers is made. Furthermore, the beam forming weights are not adapted to the external angular spectrum but rather fixed. The actual signals received on the various beams are, of course, determined by the incident angular spectrum.

The channel "slowing" is demonstrated in Figs. 1–4. In Fig. 1, the beam patterns of four beams that may be formed by a linear array of four antennas are shown. The antenna elements are assumed separated by $\lambda/2$ and placed on a back plane (e.g., back of a laptop), restricting the beam patterns to a half space. The beams are mutually orthogonal, except for beam 4, pointing at 40°, chosen so as not to point in the end-fire direction where the beam is naturally broader. The total Doppler spectrum observed at one antenna is plotted in Fig. 2. The plane waves are assumed to be equiprobable over a half space, resulting in only positive Doppler shift frequencies. In this simulation the array is moving with the broadside direction along the direction of motion. The Doppler spectra on the four beam-formed signals are plotted in Fig. 3, exhibiting the band limited property seen in

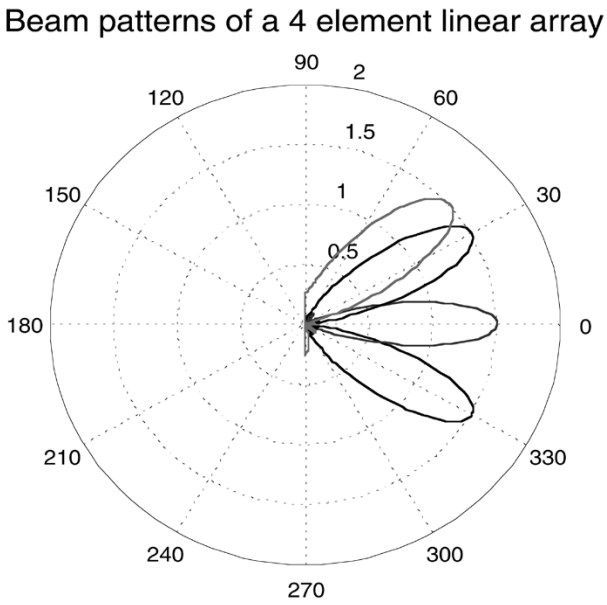

Fig. 1. Beam patterns for a four-antenna linear array, with antenna elements placed on a backplane and spaced by $\lambda/2$.

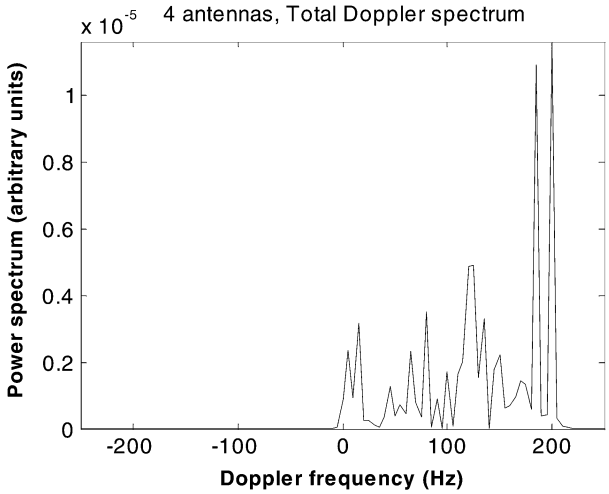

Fig. 2. Total Doppler spectrum observed at 1 antenna at 60 mph.

$$\mathbf{r}'' \approx \mathbf{D}_\mathbf{1}^\dagger(\mathbf{v}t)\mathbf{r}' = \mathbf{D}_\mathbf{1}^\dagger(\mathbf{v}t)\mathbf{B}_\mathbf{1}^\dagger\mathbf{r} = \frac{G_0\sqrt{N_R}}{\sqrt{N_L}} \times \begin{pmatrix} \sum_{k_x=-B_h/2}^{k_x=B_h/2} A_1(\mathbf{k}+\mathbf{K_1})e^{i\mathbf{k}\bullet\mathbf{v}t} & \sum_{k_x=-B_h/2}^{k_x=B_h/2} A_2(\mathbf{k}+\mathbf{K_1})e^{i\mathbf{k}\bullet\mathbf{v}t} & \cdots & \sum_{k_x=-B_h/2}^{k_x=B_h/2} A_{N_T}(\mathbf{k}+\mathbf{K_1})e^{i\mathbf{k}\bullet\mathbf{v}t} \\ \sum_{k_x=-B_h/2}^{k_x=B_h/2} A_1(\mathbf{k}+\mathbf{K}_2)e^{i\mathbf{k}\bullet\mathbf{v}t} & \sum_{k_x=-B_h/2}^{k_x=B_h/2} A_2(\mathbf{k}+\mathbf{K}_2)e^{i\mathbf{k}\bullet\mathbf{v}t} & \cdots & \sum_{k_x=-B_h/2}^{k_x=B_h/2} A_{N_T}(\mathbf{k}+\mathbf{K}_2)e^{i\mathbf{k}\bullet\mathbf{v}t} \\ \vdots & \vdots & \ddots & \vdots \\ \sum_{k_x=-B_h/2}^{k_x=B_h/2} A_1(\mathbf{k}+\mathbf{K}_{N_K})e^{i\mathbf{k}\bullet\mathbf{v}t} & \sum_{k_x=-B_h/2}^{k_x=B_h/2} A_2(\mathbf{k}+\mathbf{K}_{N_K})e^{i\mathbf{k}\bullet\mathbf{v}t} & \cdots & \sum_{k_x=-B_h/2}^{k_x=B_h/2} A_{N_T}(\mathbf{k}+\mathbf{K}_{N_K})e^{i\mathbf{k}\bullet\mathbf{v}t} \end{pmatrix} \mathbf{s} + \mathbf{D}^\dagger(\mathbf{v}t)\mathbf{B}_\mathbf{1}^\dagger\mathbf{n} \tag{25}$$

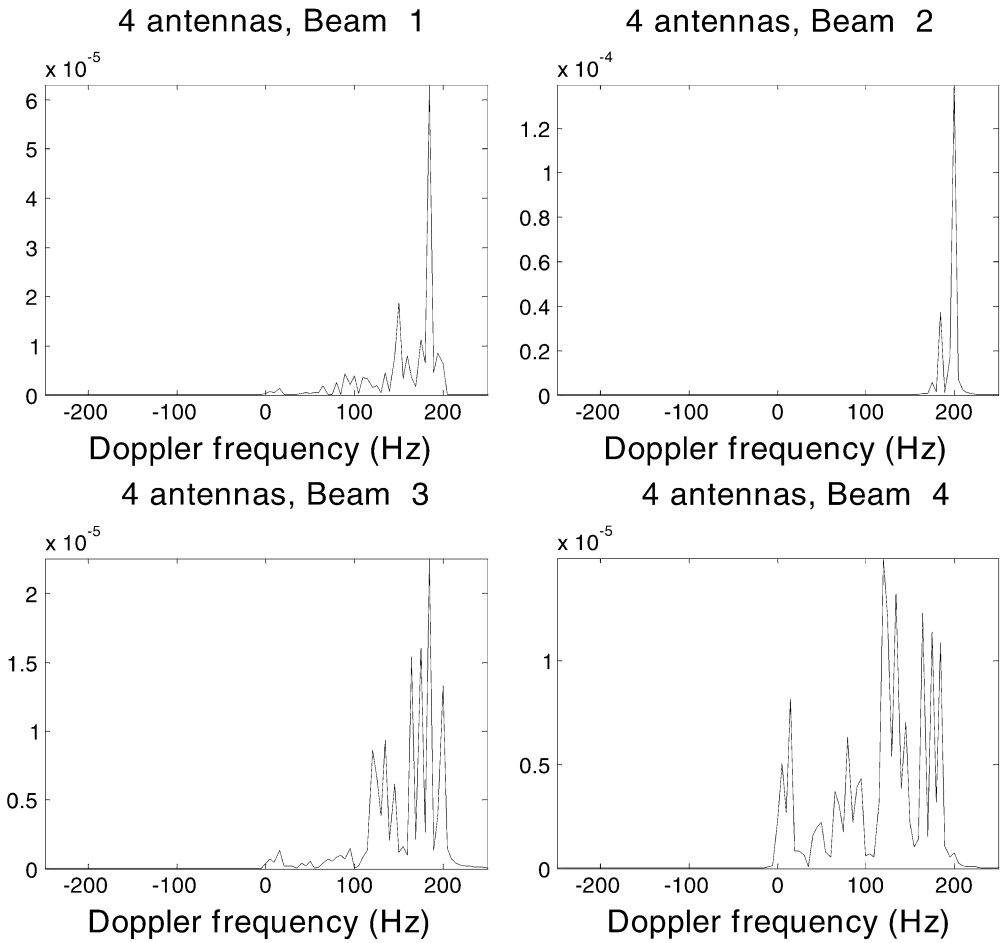

Fig. 3. Doppler spectra on four beam signals at 60 mph.

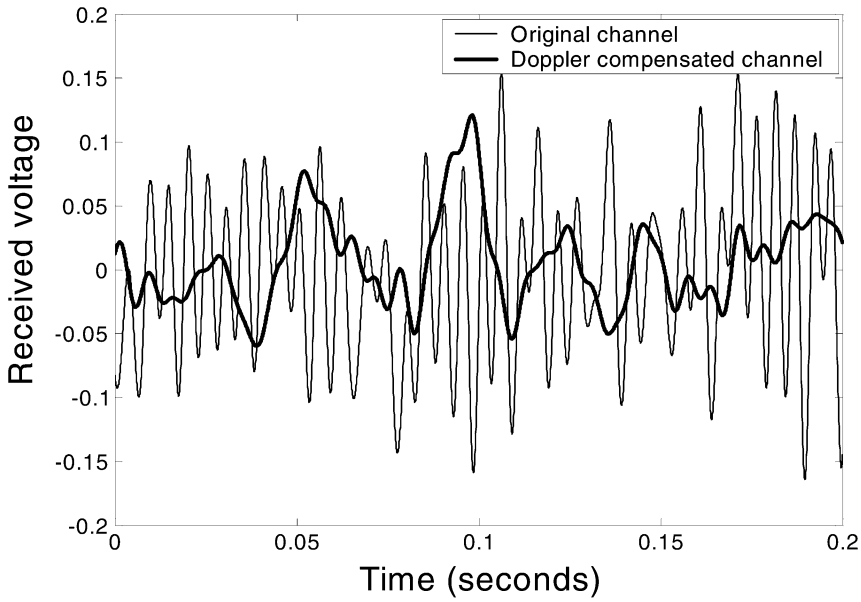

Fig. 4. Channel time-fluctuation at 60 mph. Original channel as seen on one antenna and beam-formed Doppler compensated channel on one of the beams.

(22). Beam 4 has the broadest frequency spread, as it is closest to the end-fire direction where the beams are naturally broader. Finally, the real part of the time-varying channel transfer coefficient as observed on one antenna is compared in Fig. 4 to the real part of the "slowed down" channel transfer coefficient as seen on one of the beam signals after the Doppler compensation, as in (25). The rate of channel fluctuation is significantly reduced.

V. Coherence Time for a Finite Number of Mobile Antennas

It is of interest to determine the increase in coherence time experienced by a beam-formed signal as compared to the signal received on an omnidirectional antenna. The correlation coefficient of a single $\mathbf{H}$ matrix entry $h(t)$ for a mobile moving at speed $\mathbf{v}$ in the direction indicated by angle ϕ is given by

$$\langle h(t)h^*(t+\tau)\rangle = \rho(\tau) = \int_{-\pi}^{\pi} e^{ik\mathrm{v}\tau\cos(\alpha-\phi)}p(\alpha)\,d\alpha \quad (27)$$

where the incident power angular spectrum $\mathrm{p}(\alpha)$ is normalized $\int_{-\pi}^{\pi} p(\alpha)d\alpha = 1$ and α is the angle of incidence.

Usually the coherence time is defined as the time τ_c at which the correlation coefficient has decreased to a prescribed value ρ_c from its maximum at $\tau = 0$. It may be shown that even a small error in the channel estimate leads to significant additional "channel mismatch noise." We are, therefore, interested in the case where ρ_c is approximately 1. For omnidirectional antennas, assuming the incident power spectrum is omnidirectional as well, $p(\alpha) = (1/2\pi)$ and (27) leads to [5]

$$\rho_u(\tau_u) = \rho_c = J_0(k\mathrm{v}\tau_u) \approx 1 - \left(\frac{k\mathrm{v}\tau_u}{2}\right)^2. \quad (28)$$

Here, the subscript u corresponds to the uniform angular distribution. The prescribed value of the correlation coefficient ρ_c is reached at time τ_u. Equation (28) also applies in the case of power spectrum distributed uniformly over an angular half space centered on the direction of motion. The angular receive pattern of a beam-formed phased array antenna of N_R elements is given by [7] $p(\alpha) = (\sin^2(N_R kd\sin(\alpha)/2))/(N_R^2\sin^2(kd\sin(\alpha)/2))$. The main lobe of the antenna pattern may be shown to be closely approximated as a Gaussian beam of the same root mean square (rms) angular width for analytical convenience

$$p(\alpha) = \frac{1}{\sqrt{2\pi}\sigma}\exp\left(-\frac{\alpha^2}{2\sigma^2}\right). \quad (29)$$

For narrow rms angular spread σ, the largest Doppler spread, i.e., the fastest fluctuation, occurs for motion perpendicular to the direction of beam maximum. Correspondingly, setting $\phi = 90^\circ$ in (27), the correlation coefficient becomes

$$\rho_G(\tau) = \int_{-\pi}^{\pi} e^{ik\mathrm{v}\tau\sin\alpha}p(\alpha)d\alpha \approx \int_{-\pi}^{\pi} e^{ik\mathrm{v}\tau\alpha}p(\alpha)d\alpha = \exp\left(\frac{-(k\mathrm{v}\tau\sigma)^2}{2}\right) \quad (30)$$

Here, the subscript G corresponds to the Gaussian angular spectrum. The prescribed value of the correlation coefficient ρ_c is reached at time τ_G, obtained by approximating (30) for small τ

$$\rho_G(\tau_G) = \rho_c = \exp\left(\frac{-(k\mathrm{v}\sigma\tau_G)^2}{2}\right) \approx 1 - \frac{(k\mathrm{v}\sigma\tau_G)^2}{2}. \quad (31)$$

The increase in coherence time due to beam forming may be obtained by equating (28) and (31), and finding the ratio of coherence times τ_G and τ_u :

$$\frac{\tau_G}{\tau_u} = \frac{1}{\sqrt{2}\sigma} = \frac{2.4}{\sqrt{2}\alpha_h} = \frac{2.4k}{\sqrt{2}B_h} \approx \frac{1}{\sqrt{2}}\frac{2.4N_R d}{0.886\lambda} \approx \frac{2N_R d}{\lambda} = N_R \quad (32)$$

where $\alpha_h = 2.4\sigma$ (for a Gaussian beam) is the half-power beam width in radians, B_h is approximated by (23), and the antenna separation d is set to $\lambda/2$. It may be observed from (23) and (32) that the coherence time increases linearly with the number of mobile antennas. Achievable beam width generally decreases with the number of mobile antennas and depends on the beam steering direction φ. For beams that are steered within 45° of broadside, the beam width is reasonably approximated by (23). In Fig. 5, the correlation coefficient for an omnidirectional antenna is compared to the correlation coefficient for a beam formed antenna with 25° half-power beam width pointing at 45° with respect to the direction of motion. A beam with this width may be formed by using a linear array of four antennas spaced $\lambda/2$ apart. Note from (27) that the coherence time τ appears in the correlation coefficient in a product with mobile speed. Consequently, for a particular value of ρ_c, the increase in coherence time due to beam forming and Doppler compensation at a particular speed may be used to increase the allowed vehicle speed. This would allow the same level of channel estimation and training performance at higher vehicle speed. In the limit of an infinite number of mobile antennas, the effective channel becomes locally static, provided mobile motion was the only source of temporal fluctuation.

VI. Optimal Number of Transmit Antennas

It has been pointed out by Marzetta [1], Marzetta and Hochwald [2], and Hassibi and Hochwald [3] that the optimal number of transmit antennas is limited by the coherence time of the channel. This result was obtained in the context of arbitrary form of fading, which was approximated as a block-fading process, of block duration T, which is set here to be the same as the coherence time of the channel. It was further assumed that training symbols were time-multiplexed with message symbols. Training issues for continuously fading channels were explored by Sun, Lozano, and Huang [4], again for arbitrary forms of fading processes. This section explores how the fading process implied by (5)–(7) modifies the conclusions reached in these works.

First, the argument in [1] is reproduced. Marzetta has shown that the required training interval T_τ grows approximately linearly with the number of transmit antennas M, thus $T_\tau = \alpha M$, for some constant α, and this leaves $T_d = T - T_\tau = T - \alpha M$ time available for sending the data. Foschini [2] has shown that in complex Gaussian i.i.d. channels, the capacity C in units of bits per symbol is approximately proportional to $\min(M, N_R)$. Here, we consider systems where $M \leq N_R$, thus $C = \gamma M$ for some constant γ, which depends, among other things, on the

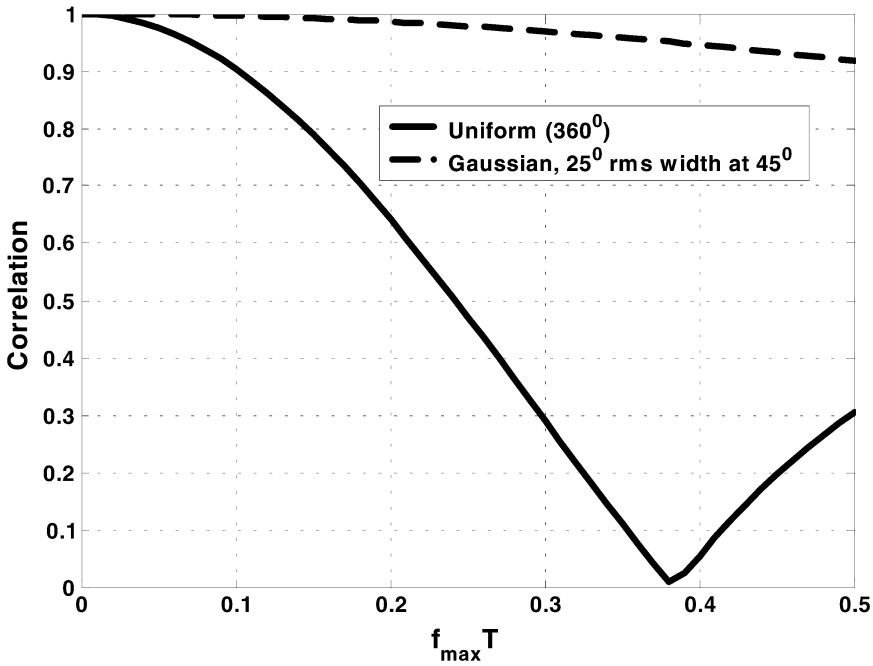

Fig. 5. Plot of temporal correlation coefficient vs. normalized time f_{max} T, where $f_{\max} = f_0 \mathrm{v}/c$ is the maximum Doppler shift frequency of the mobile moving with speed v, and T is the actual time.

SNR and N_R. Taking the view that the need for training imposes an overhead penalty by reducing the time available for sending the data, the total number of data bits that can be sent is equal to $C(T_d)/(T) = \gamma M((T - \alpha M))/(T)$. The optimum number of transmit antennas from the standpoint of maximizing the number of data bits is $M = (T)/(2\alpha)$, implying that the training interval is $T_\tau = T/2$. This analysis assumes that the coherence time of the channel is a fixed quantity, independent of the antenna array. It follows from (23) and (32) that the coherence time increases linearly with the number of mobile antennas, $T = \beta N_R$. This is approximately true for linear arrays, which are steered in directions within $\pm 45^\circ$ from broadside. The number of message bits that can be sent becomes

$$\mathrm{C}\frac{T_d}{T} = \gamma M \frac{(T - \alpha M)}{T} = \gamma M \frac{(\beta N_R - \alpha M)}{\beta N_R}. \tag{33}$$

Setting the number of receive antennas N_R as proportional to the number of transmit antennas M, $N_R = \kappa M$, (33) becomes

$$\begin{aligned}\mathrm{C}\frac{T_d}{T} &= \gamma M \frac{(\beta N_R - \alpha M)}{T} = \gamma M \frac{(\beta \kappa M - \alpha M)}{\beta \kappa M} \\ &= \gamma M \frac{(\beta \kappa - \alpha)}{\beta \kappa}.\end{aligned} \tag{34}$$

Equation (34) indicates that capacity increases linearly with number of transmit antennas M, provided the number of mobile receive antennas N_R increases proportionally. In contrast to the result in [1], there is no finite optimum number of transmitting antennas. This argument is tempered by the fact that, in general, mobile motion is not the only source of temporal fading. Motion of scatterers, such as trees swaying in the wind, other vehicles, and pedestrians would induce channel fluctuations that are not represented by the model in (5)–(7). Another source of temporal channel fluctuation is the large-scale fading, experienced by the mobile as it traverses distances, which are larger than the spatial scale over which the angular spectrum may be assumed to be homogeneous (e.g., moving through a city block). These effects would still limit the optimum number of transmit antennas, as per [1], albeit on a much longer temporal scale. Nevertheless, it is generally recognized that mobile motion is the primary source of rapid temporal channel fluctuation, and MIMO channel estimation limits the maximum allowed vehicle speed. Reduction of perceived speed through beam forming and Doppler compensation would alleviate this constraint. As the number of mobile receive antennas increases, the number of channel coefficients that is estimated increases correspondingly. This presents, at most, a computational burden, but not a fundamental difficulty in estimation, as each beam space receiver needs to estimate channels from M transmitters and a single Doppler frequency. Note that for each mobile receive beam, all transmit antennas suffer the same mean Doppler shift, thus the need to estimate only a single Doppler frequency per mobile receive beam, regardless of the number of base transmit antennas. To illustrate the easing of the estimation difficulties, the number of parameters that needs to be estimated per unit time is examined. In the absence of beam forming, each receiver has to estimate M complex channel coefficients in the coherence time $T\lambda/(2\mathrm{v})$ of the channel, so the "learning rate" is $2M/T$ real numbers/second for each receiver. In contrast, each of the beam space receivers needs to estimate the coefficient of the "slowed" channel at the rate of $(2M)/(N_R T)$ $(=2/T$, for $N_R = M)$ real numbers/second and a single mean Doppler frequency. The total number of parameters to estimate per second is $2M/T$, but additional receivers bring more received signals, thus increasing the computational burden but not the estimation error. The Doppler frequency changes at the rate of vehicle acceleration/deceleration, a slow rate neglected here. It is tacitly assumed here that as the number of mobile antennas grows, the channel characteristics observed by each are statistically identical. As the size of the

mobile array grows, shadow fading variations from antenna to antenna may become significant. This is expected to occur when array size reaches a scale of several meters or larger. There is no attempt in this work to extend the analysis to such mobile array sizes. It may be noted that moving an array of such size through a cluttered environment may present logistical and safety difficulties.

VII. Uplink Beam Forming at the Mobile Transmitter

Ordinarily in MIMO communication, a separate information stream is sent from each mobile transmitter, resulting in Doppler spreads identical to those experienced on the downlink. The earlier ideas may be used at the mobile transmitter as well to slow the apparent channel fluctuations. By reciprocity, the uplink channel matrix is a transpose of the downlink channel matrix (7), evaluated at the appropriate uplink center frequency f^U

$$\mathbf{H}(t, f^U) = \mathbf{H}_k^T(f^U)\mathbf{D}(f^U, \mathbf{v}t)\mathbf{B}^T(f^U) \tag{35}$$

where the superscript T stands for nonconjugate transpose. In the case of the downlink, the beam forming transformation $\mathbf{B}_\mathbf{1}^\dagger$ (18) was applied to the signal vector received at the mobile. For the uplink, we wish to send out each transmitted signal from the mobile along a "beam." The transformation needed to accomplish this may be obtained by inverting the beam forming transformation $\mathbf{B}_\mathbf{1}^\dagger$ (here, assumed to be square), followed by phase-conjugation required to reverse the direction of propagation from incoming to outgoing. The transformation applied to the source signal vector $\mathbf{s}$ is thus $[(\mathbf{B}_\mathbf{1}^\dagger)^{-1}]^*$. When the beams are constructed as orthogonal beams, the matrix $\mathbf{B_1}$ is unitary, thus $[(\mathbf{B}_\mathbf{1}^\dagger)^{-1}]^* = \mathbf{B}_\mathbf{1}^* = (\mathbf{B}_\mathbf{1}^\dagger)^T$. Each signal should be precompensated for Doppler prior to beam forming. The actual transmitted signal vector $\mathbf{x}$ is then related to the original source signal vector $\mathbf{s}$ by

$$\mathbf{x} = \left(\mathbf{B}_\mathbf{1}^\dagger\right)^T \mathbf{D}_1^\dagger(f_U, \mathbf{v}t)\mathbf{s}. \tag{36}$$

Using (36) as a source in channel (35), leads to an uplink received signal

$$\begin{aligned}\mathbf{r} &= \mathbf{H}(t, f^U)\mathbf{x} + \mathbf{n} \\ &= \mathbf{H}_k^T(f^U)\mathbf{D}(f^U, \mathbf{v}t)\mathbf{B}^T(f^U) \\ &\quad \times \left(\mathbf{B}_\mathbf{1}^\dagger\right)^T \mathbf{D}_1^\dagger(f_U, \mathbf{v}t)\mathbf{s} + \mathbf{n}.\end{aligned} \tag{37}$$

The effective channel in (37) may be shown to have been "slowed down" through an analysis similar to that in Section IV. Note that in the case of the mobile antenna array mounted externally to the vehicle, the beam forming matrix $\mathbf{B}_1$ defined in (18), as well as the Doppler compensation matrix $\mathbf{D}_1$, defined in (22), consist of phase shift elements that depend in a simple manner on signal frequency f through the wavenumber $|\mathbf{k}| = k = 2\pi f/c$. Both beam forming and Doppler compensating phase shifts, learned on the downlink, may be rescaled to accommodate a different frequency of operation for the uplink by multiplying the phase of each matrix entry by the ratio of center frequencies f_0^U/f_0^D. The frequency selectivity of the channel is still retained within the matrix factor $\mathbf{H}_k(f)$, which may be dramatically different for uplink and downlink frequencies, as in frequency division duplex (FDD) systems. The "slowing down" may, therefore, be carried out in uplink transmission without relying on complete knowledge of the uplink channel.

Effective use of downlink beam forming weights for the uplink requires calibration between the receiver and transmitter chains. No assumption is made here that beam forming has led to a reduction in delay spread.

In cases when there is significant scattering in the immediate vicinity of the mobile, as within a vehicle, beam forming weights appropriate for downlink reception are different than those indicated in (18). This would, in general, make the procedure of rescaling the downlink reception weights to derive uplink transmission weights at the mobile array inappropriate.

VIII. Conclusion

In this paper, the MIMO channel is represented in terms of a sum of plane waves incident at the mobile. The channel transfer matrix is found to factor into time-dependent and time-independent parts. It is then proposed that the received signals are first preprocessed so as to produce signals that fluctuate on a much slower time scale. The preprocessing consists of beam forming and Doppler compensation for signals received on each beam. Both operations are nonsingular and do not alter the capacity of the MIMO channel. This is shown to effectively "slow down" the channel fluctuation due to mobile motion. The coherence time of the preprocessed channel is found to increase by a factor on the order of the number of mobile receive antennas. In the limit of an infinite number of mobile receive antennas, the effective MIMO channel is shown to become locally static. These results remove constraints on the number of transmit antennas and allowed vehicle speeds imposed by training requirements. The "slowed down" channel may also be fed back to the transmitter, allowing an increase in information throughput.

Acknowledgment

The author is grateful to C. Papadias and J. Foschini for early discussions that proved invaluable to this work. He would like to thank A. Lozano and J. Saltz for their helpful comments on the draft of this work. Extensive discussions with S. Venkatesan, L. Mailender, and R. Valenzuela were crucial in assessing the applicability of this work. The author would also like to acknowledge discussions with M. Gans, I. Korisch, H. Xu, J. Ling, and D. Samardzija, as well as useful suggestions by reviewers and the editor.

References

[1] T. L. Marzetta, "BLAST Training: Estimating channel characteristics for high capacity space-time wireless," in *Proc. 37th Annu. Allerton Conf. Communication, Control, Computing*, Monticello, IL, Sept. 22–24, 1999.

[2] T. L. Marzetta and B. M. Hochwald, "Fundamental limitations on multiple-antenna wireless links in Rayleigh fading," *Proc. IEEE Int. Symp. Information Theory*, p. 310, 1998.

[3] B. Hassibi and B. M. Hochwald, "How much training is needed in multiple-antenna wireless links?," *IEEE Trans. Inform. Theory*, submitted for publication.

[4] Q. Sun, D. C. Cox, A. Lozano, and H. C. Huang, "Training-based channel estimation for continuous flat fading blast," in *Proc. IEEE Int. Conf. Communications*, New York, NY, Apr. 2002.
[5] W. C. Jakes, *Microwave Mobile Communications*. New York: IEEE Press, 1974.
[6] D. Chizhik, G. J. Foschini, and R. A. Valenzuela, "Capacities of multi-element transmit and receive antennas: Correlations and Keyholes," *IEE Electron. Lett.*, vol. 36, no. 13, pp. 1099–1100, June 22, 2000.
[7] W. L. Stutzman and G. A. Thiele, *Antenna Theory and Design*. New York: Wiley, 1981.
[8] A. L. Moustakas, S. Arunachalam, K. H. Wu, and H. Heller, "Wide-band spatio-temporal characterization of the urban PCS channel," ITD-01-41 387L.
[9] H. Xu, M. Gans, D. Chizhik, J. Ling, P. Wolniansky, and R. Valenzuela, "Spatial and temporal variations of MIMO channels and impacts on capactity," in *Proc. IEEE Int. Conf. Communications*, Apr. 2002, pp. 262–266.
[10] D. Smardzija and N. Mandayam, "Pilot assisted MIMO channel estimation and achievable rates," in *Proc. DIMACS Workshop Signal Processing for Wireless Transmission*. Piscataway, NJ, Oct. 7–9, 2002.
[11] D.-S. Shiu, G. J. Foschini, M. J. Gans, and J. M. Kahn, "Fading correlation and its effect on the capacity of multielement antenna systems," *IEEE Trans. Commun.*, vol. 48, pp. 502–513, Mar. 2000.
[12] D. Chizhik, F. Rashid-Farrokhi, J. Ling, and A. Lozano, "Effect of antenna separation on the capacity of BLAST in correlated channels," *IEEE Commun. Lett.*, vol. 4, pp. 337–339, Nov. 2000.
[13] K. I. Pedersen, J. B. Andersen, J. P. Kermoal, and P. Mogensen, "A stochastic multiple-input-multiple-output radio channel model for evaluation of space-time coding algorithms," in *Proc. IEEE Vehicular Technology Conf.*, vol. 2, 2000, pp. 893–897.
[14] A. M. Sayeed, "Deconstructing multiantenna fading channels," *IEEE Trans. Signal Processing*, vol. 50, pp. 2563–2579, Oct. 2002.
[15] M. Steinbauer, A. F. Molisch, and E. Bonek, "The double-directional radio channel," *IEEE Antennas Propagat. Mag.*, vol. 43, pp. 51–63, Aug. 2001.
[16] O. Norklit and R. G. Vaughan, "Angular partitioning to yield equal Doppler contributions," *IEEE Trans. Veh. Technol.*, vol. 48, no. 5, pp. 1437–1442, Sept. 1999.
[17] G. J. Foschini and M. J. Gans, "On limits of wireless communications in a fading environment when using multiple antennas," *Wireless Personal Commun.*, vol. 6, p. 311, Mar. 1998.
[18] G. J. Foschini, "Layered space-time architecture for wireless communication in a fading environment when using multiple antennas," *Bell Labs Tech. J.*, vol. 1, no. 2, pp. 41–59, Autumn 1996.
[19] H. Asplund, A. F. Molisch, M. Steinbauer, and N. B. Mehta, "Clustering of scatterers in mobile radio channels-evaluation and modeling in the COST259 directional channel model," in *Proc. IEEE Int. Conf. Communications*, vol. 2, 2002, pp. 901–905.
[20] A. M. Sayeed and V. V. Veeravalli, "Essential degrees of freedom in time and frequency selective MIMO channels," in *Proc. 5th Int. Symp. Wireless Personal Multimedia Communications*, vol. 1, 2002, pp. 107–111.

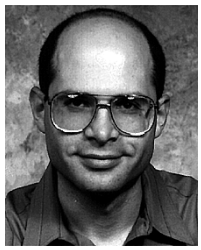

Dmitry Chizhik received the Ph.D. degree in electrophysics from the Polytechnic University, Brooklyn, NY. His thesis work focused on ultrasonics and nondestructive evaluation.

He joined the Naval Undersea Warfare Center, New London, CT, where he did research in scattering from the ocean floor, geoacoustic modeling, and shallow water acoustic propagation. In 1996, he joined Bell Laboratories, Holmdel, NJ, where he has been working on radio propagation modeling and measurements, using deterministic and statistical techniques. His recent work has been in measurement, modeling and channel estimation of MIMO channels. The results are used both for determination of channel-imposed bounds on channel capacity, system performance, as well as for optimal antenna array design. His research interests include acoustic and electromagnetic wave propagation, signal processing, and communications.